2018

High-Sensitivity Salinity Sensor Based on Optical Microfiber Coil Resonator

Y. YIN
College of Science, Harbin Engineering University, Harbin 150001, China

S. LI
College of Science, Harbin Engineering University, Harbin 150001, China

J. REN
College of Science, Harbin Engineering University, Harbin 150001, China

See next page for additional authors

Recommended Citation

Wang, P. et al. (2018) High-Sensitivity Salinity Sensor Based on Optical Microfiber Coil Resonator, Vol. 26, No. 26 | 24 Dec 2018 | *OPTICS EXPRESS* 34634 doi:10.1364/OE.26.034633

Research Article | Vol. 26, No. 26 | 24 Dec 2018 | OPTICS EXPRESS 34633
Optics EXPRESS

High-sensitivity salinity sensor based on optical microfiber coil resonator

Y. YIN,[1] S. LI,[1] J. REN,[1] G. FARRELL,[2] E. LEWIS,[3] AND P. WANG [1,4,*]

[1]*Key Laboratory of In-fiber Integrated Optics of Ministry of Education, College of Science, Harbin Engineering University, Harbin 150001, China*
[2]*Photonics Research Centre, Dublin Institute of Technology, Kevin Street, Dublin 8, Ireland*
[3]*Optical Fibre Sensors Research Centre, Department of Electronic and Computer Engineering, University of Limerick, Limerick, Ireland*
[4]*Key Laboratory of Optoelectronic Devices and Systems of Ministry of Education and Guangdong Province, College of Optoelectronic Engineering, Shenzhen University, Shenzhen 518060, China*
[*]*pengfei.wang@dit.ie*

Abstract: A simple, compact, and high-sensitivity optical sensor for salinity measurement is reported based on an optical microfiber coil resonator (MCR). The MCR is manufactured by initially wrapping microfiber on a polymethylmethacrylate (PMMA) rod, which is dissolved to leave a hollow cylindrical fluidic channel within the coil for measurement. Based on the light propagation through the MCR, the device's spectrum moves to long wavelengths with increased salinity in the fluid. The MCR device's sensitivity can reach up to 15.587 nm/% with a resolution of 1.28×10^{-3}%. It is also confirmed that the temperature dependence is 79.87 pm/°C, which results from the strong thermal-expansion coefficient of the low refractive index epoxy. The experimental results indicate that the device can be widely used as a high sensitivity salinity sensor in water and other liquids due to its stability, compactness, electromagnetic immunity, and high sensitivity.

1. Introduction

In recent years, salinity sensing has attracted much attention in potential areas ranging from marine monitoring, marine circulation, marine climate and environment protection in oceanography [1–4]. Generally, traditional methods of salinity measurement have been based on electronic methods (electrochemical) to detect the existence of chlorine ions of the seawater [5,6]. However, this method is affected greatly from the harsh environment, such as high corrosivity, extreme temperature and strong electromagnetic interference and is not used widely in micro scale due to its large size and complex structure. Electrochemical sensors are also prone to cross-sensitivity from and can even be damaged by other species e.g. nitrates (from Agriculture) and Sulphuric compounds (e.g. from dissolved SO_2) Therefore, there is a clear need for new sensors with compact size, high stability, good selectivity and electromagnetic immunity.

Optical Microfibres have been widely applied for salinity sensing because of the excellent light matter interaction developed via the strong evanescent field surrounding the microfiber. Salinity sensors based on microfibre have attracted particular attention due to their advantages of compact size, low loss, low cost and electromagnetic immunity [7–9]. Existing forms of salinity sensor based on microfibre include a Mach-Zehnder interferometer [10], a microfibre loop [8], a Bragg grating [11] and a direction coupler [9]. Among the numerous devices based on microfibre, the microfibre resonator represents a significant development in the field of evanescent wave sensing. The microfibre coil resonator (MCR) therefore has great potential in the general optical sensing field and has been used for measurement of refractive index [12], temperature [13] and electric current [14]. However, to the best of our knowledge, there is no experimental work on the salinity sensing by an MCR so far.

#348781 https://doi.org/10.1364/OE.26.034633
Journal © 2018 Received 22 Oct 2018; revised 5 Dec 2018; accepted 7 Dec 2018; published 20 Dec 2018

Optics EXPRESS

In this paper, a salinity sensor based on an MCR is fabricated by wrapping a microfibre on a polymethylmethacrylate (PMMA) rod covered with a UV-curable low refractive index epoxy and dissolving the PMMA rod to constitute a fluidic channel. The light propagation of the MCR is sensitive to the refractive index of its surrounding environment, so the device based on the MCR is very applicable to salinity sensing in fluids. The resonance wavelength moves towards long wavelengths in the presence of increasing salinity and the device exhibits a high sensitivity of 15.5874 nm/% and a temperature dependence of 0.07987 nm/°C. The latter is present due to the strong thermal-expansion coefficient caused by the low refractive index epoxy. The demonstrated sensor provides a novel method to measure salinity and offers a good reference for salinity measuring for use in other fields, including chemistry and biology.

2. Theory

According to the analysis of Sumetsky [15], the light propagation around an MCR with n turns is described by the following equations:

$$-i\frac{d}{ds}\begin{bmatrix} A_1(s) \\ A_2(s) \\ A_3(s) \\ \vdots \\ A_{n-2}(s) \\ A_{n-1}(s) \\ A_n(s) \end{bmatrix} = \begin{bmatrix} 0 & k & 0 & 0 & \cdots & 0 & 0 & 0 \\ k & 0 & k & 0 & \cdots & 0 & 0 & 0 \\ 0 & k & 0 & k & \cdots & 0 & 0 & 0 \\ \vdots & \vdots & \vdots & \vdots & \vdots & \vdots & \vdots & \vdots \\ 0 & 0 & 0 & 0 & \cdots & 0 & k & 0 \\ 0 & 0 & 0 & 0 & \cdots & k & 0 & k \\ 0 & 0 & 0 & 0 & \cdots & 0 & k & 0 \end{bmatrix} \begin{bmatrix} A_1(s) \\ A_2(s) \\ A_3(s) \\ \vdots \\ A_{n-2}(s) \\ A_{n-1}(s) \\ A_n(s) \end{bmatrix} \tag{1}$$

where $A_m(s)$ is the varying amplitude of the electric field at the m^{th} coil with a distance s around the coil, and k is the coupling coefficient between adjacent coils. For the propagation in the MCR, the output amplitude at the end of the m^{th} coil is equal to the input amplitude at the beginning of the $(m + 1)^{th}$ coil, which implies the following continuity condition:

$$\begin{bmatrix} A_1(0) \\ A_2(0) \\ A_3(0) \\ \vdots \\ A_{n-2}(0) \\ A_{n-1}(0) \\ A_n(0) \end{bmatrix} = \begin{bmatrix} 0 & 0 & 0 & \cdots & 0 & 0 & 0 \\ \exp^{i\beta S} & 0 & 0 & \cdots & 0 & 0 & 0 \\ 0 & \exp^{i\beta S} & 0 & \cdots & 0 & 0 & 0 \\ \vdots & \vdots & \vdots & \vdots & \vdots & \vdots & \vdots \\ 0 & 0 & 0 & \cdots & 0 & 0 & 0 \\ 0 & 0 & 0 & \cdots & \exp^{i\beta S} & 0 & 0 \\ 0 & 0 & 0 & \cdots & 0 & \exp^{i\beta S} & 0 \end{bmatrix} \begin{bmatrix} A_1(S) \\ A_2(S) \\ A_3(S) \\ \vdots \\ A_{n-2}(S) \\ A_{n-1}(S) \\ A_n(S) \end{bmatrix} + \begin{bmatrix} A_1(0) \\ 0 \\ 0 \\ \vdots \\ 0 \\ 0 \\ 0 \end{bmatrix} \tag{2}$$

where β is the propagation constant of the fundamental mode (HE_{11}) and S is the length of each coil. The input of the MCR is determined by $A_1(0)$ while the output of the MCR is given by $A_n(S)\exp(i\beta S)$. The amplitude transmittance of the MCR is defined as:

$$T = \frac{A_n(S)\exp(i\beta S)}{A_1(0)} \tag{3}$$

Note that β in the Eq. (3) is defined as an imaginary propagation constant $\beta = 2\pi/\lambda + i\alpha$, where α represents the optical loss of the microfibre.

The output light intensity of the MCR can be expressed as:

$$I = T \times T^* \tag{4}$$

Optics EXPRESS

where T^* is the complex conjugate of T.

To investigate the dependence of the output light intensity on salinity, a salinity sensing mode based on the MCR is established. The eigenvalue equation for HE_{11} is given by [16]:

$$\left\{\frac{J_1'(U)}{UJ_1(U)}+\frac{K_1'(W)}{WK_1(W)}\right\}\left\{\frac{J_1'(U)}{UJ_1(U)}+\frac{n_2^2K_1'(W)}{n_1^1WK_1(W)}\right\}=(\frac{\beta}{kn_1})^2(\frac{V}{UW})^4 \quad (5)$$

where n_1 is the refractive index (RI) of the fibre, n_2 is the RI of the salt solution, $k=2\pi/\lambda$, d is the diameter of fibre, J_1 is the Bessel function of the first kind and K_1 is the modified Bessel function of the second kind. The modelling results in transmission spectra which vary with different salinities and are shown in Fig. 1(a). The refractive index of the salt solution as a function of salinity was measured and was found to have a linear relationship, expressed by the formula: $y=0.00192x+1.33397$, where y is the refractive index and x is the salinity. When light propagates in the MCR, the refractive index of the salt solution will change the output light intensity and in turn this will alter the transmission spectrum. Since the salinity affects the refractive index, the salinity level will therefore affect the transmission spectrum. With a suitable calibration of the changes in the transmission response it is possible to measure the salinity. The resonance wavelength experiences a red-shift with the increasing of salinity concentration.

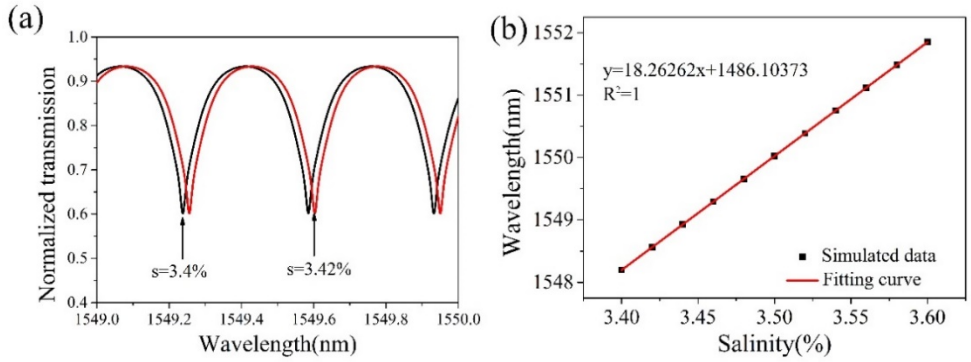

Fig. 1. (a) Normalized transmission spectra at two different salinities. (b) Theoretical relationship between resonance wavelength and salinity.

Based on the above modeling, a theoretical study on the dependence of the resonance wavelength on salinity is performed and the calculation result is plotted as the red line in Fig. 1(b). It shows that the resonance wavelength increases linearly with increasing of salinity and the slope is 18.26262 nm/%.

3. Experiment

The fabrication process for the salinity sensor based on the MCR is described in this section. Initially, a microfibre was fabricated by drawing a standard commercial single-mode fibre (SMF-28) when heated by a small ceramic heater [17] and the diameter of microfibre is 2.32 μm. The fabricated microfibre was wrapped around a 1mm-diameter PMMA rod as shown in Fig. 2(a) (Goodfellow, ME307901), covered with a UV-curable low refractive index epoxy (Luvantix, PC373) and fully cured using a UV lamp (Lightningcure, LC8) to reduce any unnecessary loss caused by the difference in refractive index between the PMMA and the microfibre. The gap between adjacent coils was 7.36 μm and the supporting rod diameter after it is covered with the low refractive index epoxy is 1.3 mm. The MCR was subsequently packaged with the same UV-curable low refractive index epoxy and fully cured using the same UV lamp. In order to enhance the mechanical stability, the fabricated MCR was placed on a glass slide (BK7) coated with the same UV-curable low refractive index epoxy and again

Optics EXPRESS

fully cured. Finally, the MCR was immersed into acetone for 12 hours to dissolve the PMMA support rod which resulted in the device which incorporates a hollow cylindrical channel structure. The PMMA rod covered with a UV-curable low refractive index epoxy and with the MCR fibre in place sits on glass slide which is inverted into a small beaker (5 mL) filled with acetone so that the PMMA rod is immersed completely and dissolves slowly. Acetone was added to the beaker every three hours to account for the loss of acetone due to vaporisation. After 12 hours, the PMMA rod was dissolved completely and a hollow cylindrical channel is formed. The proposed salinity sensor used a 4-turn MCR and a fluidic channel surrounded by low refractive index epoxy was obtained with the completion of the step described above.

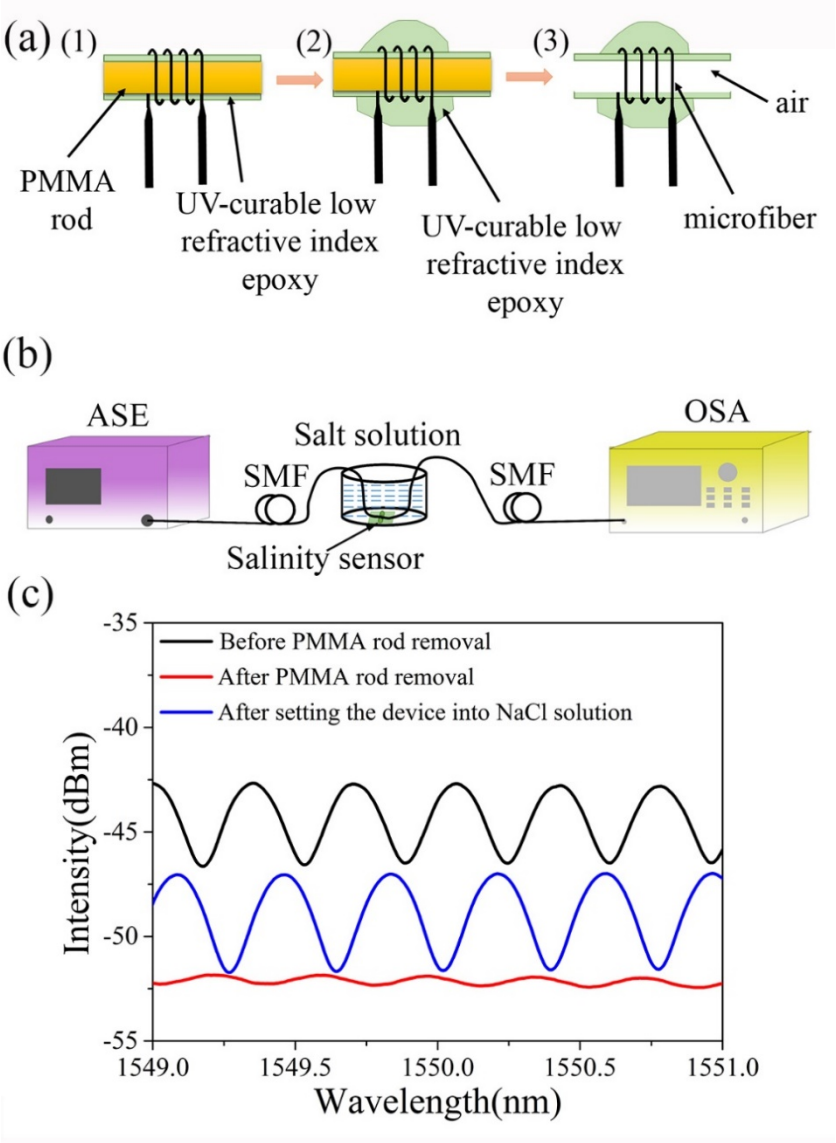

Fig. 2. (a) Fabrication process of the salinity sensor. (b) Schematic diagram of the experiment system. (c) Transmission spectra of the MCR before and after removal the PMMA rod and after setting into salt solution.

Optics EXPRESS

The proposed experimental system was established shown in Fig. 2(b). The spectral characteristics were investigated using this system which comprised a broadband amplified spontaneous emission (ASE) source (YSL SC-series) connected to the input fibre and an optical spectrum analyzer (OSA) (YOKOGAWA, AQ-6370C) connected to the output fibre. The salinity sensor was immersed into a salt (Sodium Chloride) solution sample with a salinity of 3.4640%, which was based on a mixture of deionized water and dissolved salt. The transmission spectra of the sensor before the PMMA rod was dissolved, after the PMMA rod was dissolved and after immersing the sensor into the salt solution are depicted in Fig. 2(c). The free spectral range was measured as 0.37 nm (Fig. 2(c)) and remains constant through the fabrication process. Nevertheless, the three oscillation strengths (amplitudes) are significantly changed, which indicates that the length of a single turn of the MCR is invariant so that the single coil of microfibre is not altered on formation of the fluidic channel. The variations in amplitude can be attributed to mechanical variations during the process of fabrication. Due to the fluidity and expansion of the liquid, the gap between adjacent coils changes during the process of fabrication and experiment, thus altering the coupling between each of the turns and the amplitude of transmission spectrum.

4. Analysis

The salinity sensitivity can be measured by immersing the sensor into a prepared salt solution sample and carefully changing the salinity. By adding 0.5 ml 6.98% salt solution to a 150 ml salt solution sample with a salinity of 3.4640%, the salinity of the solution increased by diffusion and dissolving into the solution. The transmission spectra measured with different salinities are shown in Fig. 3(a). It can be seen that the transmission spectra move towards the longer wavelengths linearly as the salinity increases and the spectrum shape is maintained essentially constant. The experimental result therefore agrees well with the theoretical analysis described above and shown in Fig. 1(b) (reproduced and included in Fig. 3(b)).

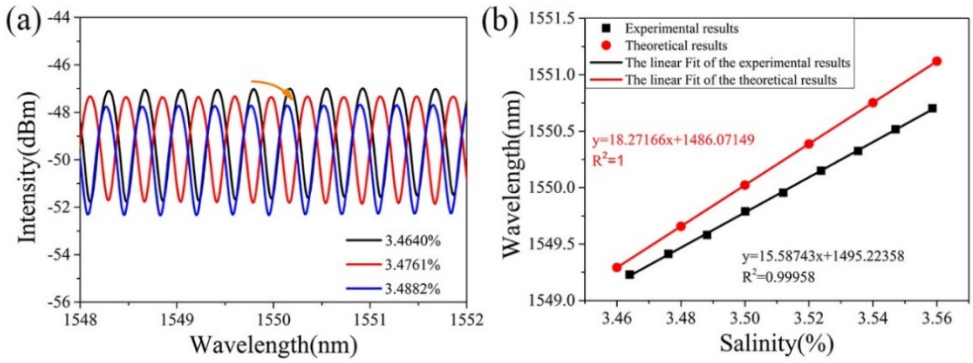

Fig. 3. (a) Transmission spectra of the salinity sensor at different salinities. (b) Experimental and theoretical relationship between resonance wavelength and salinity.

Figure 3(b) shows the variation of the resonance wavelength as a function of salinity concentration. A linear regression analysis of the experimental results yielded a high R-squared value of 0.99958, and the salinity sensitivity was found to 15.58743 nm/%, which is a little lower than the theoretical result. With the resolution of OSA of 0.02 nm, the minimum salinity change that can be distinguished is 1.28×10^{-3}%. The low value of the salinity sensitivity can be attributed to the relatively large fraction of the mode propagating in the MCR and the salt solution, and hence the effective refractive index, n_{eff} experienced by the propagating mode in the sensor will increase more slowly than predicted as a result of the existence of the low refractive index epoxy layer that exists between the microfibre and the salt solution [18]. Moreover, as the experiment progresses, the PMMA may deposit a thin residual layer on the inside wall of the fluidic channel and the roughness of the PMMA rod

Optics EXPRESS

would in turn result in a lack of smoothness of the fluidic channel. The roughness of the fluidic channel also limits the interaction length between the mode and the salt solution and hence lowers the salinity sensitivity.

In order to investigate the temperature influence on the characteristics of transmission spectra, the fabricated salinity sensor was placed inside a temperature-controlled environmental chamber (ESPEC SH-222) to measure the temperature characteristic response. The experimental layout for this test is shown schematically in Fig. 4(a). The input fibre was connected to the same broadband amplified spontaneous emission (ASE) source (YSL SC-series) and the output fibre was connected to the identical optical spectrum analyzer (OSA) (YOKOGAWA, AQ-6370C). Figure 4(b) shows the transmission spectra of the salinity sensor obtained at different temperatures. The environmental temperature was initially increased from 28 °C to 30 °C and the spectra recorded with a temperature increment of 1 °C. As shown in Fig. 4(b), the resonance wavelength moves towards the longer wavelengths as the temperature increases. Figure 4(c) shows the dependence of the resonance wavelength with temperature in the range of from 20 °C to 30 °C, and the spectra were recorded for temperature increments of 1 °C. The temperature sensitivity of the fabricated salinity sensor was determined as ~79.87 pm/°C, which indicates that temperature variation can have a significant effect on the wavelength characteristics, which can be attributed to the strong thermal-expansion coefficient (1.7×10^{-4} /°C) of the low refractive index epoxy. The influence of temperature can be reduced by replacing the low refractive index epoxy with lower thermal-expansion coefficient and modifying the fabricated parameters of the MCR including the gap between adjacent coils and the diameter of support rod [19]. Another method is utilizing the Bragg gating in the polymer optical fibre, which has negative temperature sensitivity and with a suitable interrogation scheme can counteract the high temperature dependence of the salinity sensor [20].

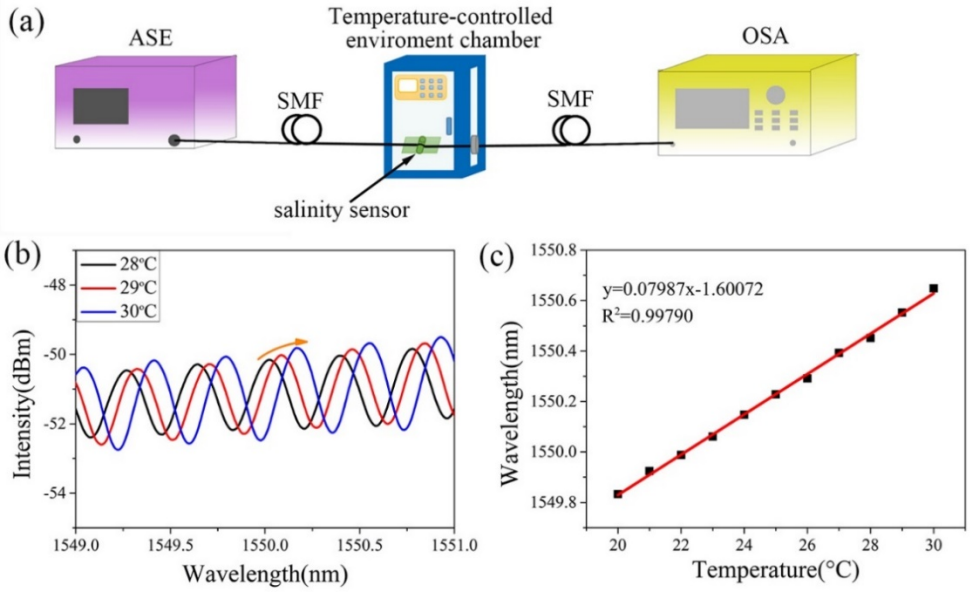

Fig. 4. (a) Schematic of the experiment set-ups for the temperature sensitivity measurement. (b) Experimental spectra of the salinity sensor at different temperature. (c) Temperature dependence of the resonance wavelength. The solid line is the linear fit to the experiment data (solid squares).

Optics EXPRESS

5. Conclusion

In conclusion, a salinity sensor based on a novel MCR design has been successfully fabricated and demonstrated. The sensor comprises a 4-turns MCR embedded in a fluidic channel of low refractive index epoxy. According to the propagation characteristics of the MCR, a theoretical mode propagation model was developed based on the resonance wavelength red-shifts with the increase of salinity. The on-line monitoring of the sensor during preparation i.e. before the PMMA rod was dissolved, after PMMA rod was dissolved and on immersing the sensor into salt solution ensures that the structure of the sensor retains stability during the fabrication process. The salinity sensitivity of 15.58743 nm/% was achieved with a fluidic channel and a four-turns MCR and the minimum resolution was 1.28×10^{-3}%. The high temperature dependence of 79.87 pm/°C is due to the strong thermal-expansion coefficient of the low refractive index epoxy. The novel MCR salinity sensor of this investigation constitutes a new optical method to measure salinity in a liquid environment and features excellent stability, compactness, electromagnetic immunity and high sensitivity, the sensor can be widely applied in salinity sensing in various fields.

Funding

National Natural Science Foundation of China (NSFC) (61575050); National Key R&D Program of China (2016YFE0126500); Key Program for Natural Science Foundation of Heilongjiang Province of China (ZD2016012); Open Fund of the State Key Laboratory on Integrated Optoelectronics (IOSKL2016KF03); 111 project (B13015) to the Harbin Engineering University.

References

1. Y. Zhao, Y. Liao, B. Zhang, and S. Lai, "Monitoring technology of salinity in water with optical fiber sensor," J. Lightwave Technol. **21**(5), 1334–1338 (2003).
2. N. Reul, S. Fournier, J. Boutin, O. Hernandez, C. Maes, B. Chapron, G. Alory, Y. Quilfen, J. Tenerelli, S. Morisset, Y. Kerr, S. Mecklenburg, and S. Delwart, "Sea surface salinity observations from space with the SMOS satellite: a new means to monitor the marine branch of the water cycle," Surv. Geophys. **35**(3), 681–722 (2014).
3. C. Gabarró, J. Font, A. Camps, M. Vall-llossera, and A. Julià, "A new empirical model of sea surface microwave emissivity for salinity remote sensing," Geophys. Res. Lett. **31**(1), 1309 (2004).
4. D. A. Pereira, O. Frazao, and J. L. Santos, "Fiber Bragg grating sensing system for simultaneous measurement of salinity and temperature," Opt. Eng. **43**(2), 299–304 (2004).
5. R. A. Cox, F. Culkin, and J. P. Riley, "The electrical conductivity/chlorinity relationship in natural sea water," Deep-Sea Res. **14**(2), 203–220 (1967).
6. G. I. Roden and J. D. Irish, "Electronic digitization and sensor response effects on salinity computation from CTD field measurements," J. Phys. Oceanogr. **5**(1), 195–199 (1975).
7. Y. Liao, J. Wang, H. Yang, X. Wang, and S. Wang, "Salinity sensing based on microfiber knot resonator," Sens. Actuators A Phys. **233**, 22–25 (2015).
8. S. Wang, J. Wang, G. Li, and L. Tong, "Modeling optical microfiber loops for seawater sensing," Appl. Opt. **51**(15), 3017–3023 (2012).
9. S. Wang, H. Yang, Y. Liao, X. Wang, and J. Wang, "High-sensitivity salinity and temperature sensing in seawater based on a microfiber directional coupler," IEEE Photonics J. **8**(4), 1–9 (2016).
10. N. Xie, H. Zhang, B. Liu, H. Liu, T. Liu, and C. Wang, "In-line microfiber-assisted Mach-Zehnder interferometer for microfluidic highly sensitive measurement of salinity," IEEE Sens. J. **18**(21), 8767–8772 (2018).
11. J. Cong, X. Zhang, K. Chen, and J. Xu, "Fiber optic Bragg grating sensor based on hydrogels for measuring salinity," Sens. Actuators B Chem. **87**(3), 487–490 (2002).
12. G. Brambilla and F. Xu, "Demonstration of a refractometric sensor based on optical microfiber coil resonator," Appl. Phys. Lett. **92**(10), 5742 (2008).
13. Y. Chen, F. Xu, and Y. Q. Lu, "Teflon-coated microfiber resonator with weak temperature dependence," Opt. Express **19**(23), 22923–22928 (2011).
14. S. Yan, B. Zheng, J. Chen, F. Xu, and Y. Lu, "Optical electrical current sensor utilizing a graphene-microfiber-integrated coil resonator," Appl. Phys. Lett. **107**(5), 53502 (2015).
15. M. Sumetsky, "Optical fiber microcoil resonators," Opt. Express **12**(10), 2303–2316 (2004).
16. L. Tong, J. Lou, and E. Mazur, "Single-mode guiding properties of subwavelength-diameter silica and silicon wire waveguides," Opt. Express **12**(6), 1025–1035 (2004).

Optics EXPRESS

17. G. Y. Chen, T. Lee, X. L. Zhang, G. Brambilla, and T. P. Newson, "Temperature compensation techniques for resonantly enhanced sensors and devices based on optical microcoil resonators," Opt. Commun. **285**(23), 4677–4683 (2012).
18. F. Xu, P. Horak, and G. Brambilla, "Optical microfiber coil resonator refractometric sensor," Opt. Express **15**(12), 7888–7893 (2007).
19. Y. Yin, J. Yu, Y. Jiang, S. Li, J. Ren, G. Farrell, E. Lewis, and P. Wang, "Investigation of temperature dependence of microfibre coil resonators," J. Lightwave Technol. **36**(20), 4887–4893 (2018).
20. X. Chen, C. Zhang, D. J. Webb, G. D. Peng, and K. Kalli, "Bragg grating in a polymer optical fibre for strain, bend and temperature sensing," Meas. Sci. Technol. **21**(9), 094005 (2010).